TiO_2 Photocatalytic Degradation of Dichloromethane: An FTIR and Solid-State NMR Study

John Borisch, Sarah Pilkenton, Matthew L. Miller, Daniel Raftery,* and Joseph S. Francisco*

H. C. Brown Laboratory, Department of Chemistry, Purdue University, West Lafayette, Indiana 47907

Received: October 10, 2003; In Final Form: March 3, 2004

The photocatalyic oxidation of dichloromethane over TiO_2 was studied using in situ FTIR and solid-state NMR (SSNMR) methods. Dichloromethane photodegradation led to the formation of a number of long-lived intermediate species including CO, HCl, phosgene, chloroform, and CCl_4 in the presence of oxygen. FTIR studies showed that the reaction rate and product distribution were strongly dependent on the oxygen concentration. Species often thought to be products in the reactions, particularly HCl, CO, and CCl_4, were found to degrade to CO_2 and H_2O under high relative oxygen concentrations. In addition, formyl chloride was identified as a new intermediate, while phosgene was found to have two production channels. SSNMR experiments showed that one of the two phosgene species resides primarily in the gas phase, while the other was associated with the surface. Additional SSNMR studies of the adsorption of dichloromethane showed that a chloromethoxyl species was formed on anatase TiO_2. SSNMR experiments were also helpful in quantifying the intermediates and products.

Introduction

Volatile organic compounds (VOCs) represent an important class of chemicals that are, unfortunately, a major source of contamination in the environment. One of the more prominent examples, dichloromethane (CH_2Cl_2), is a widespread compound that finds many uses in industrial products and processing, such as aerosols, adhesives, dry cleaning, pharmaceuticals, refrigerants, and solvents. Since the degradation of CH_2Cl_2 could potentially release chlorine into the atmosphere (and, hence, cause destruction of stratospheric ozone),there is a need for an environmentally benign and efficient means of removing it. Although a number methods for hazardous waste treatment currently exist, including incineration,[1] adsorption,[2] and bioremediation,[3−5] heterogeneous semiconductor photocatalysis[6−10] appears promising for the degradation of a number of VOCs and can provide substantial advantages over other treatment methods. The complete destruction of VOCs using photocatalytic methods can be attained at ambient temperature and pressure with significantly lower cost than comparable thermal treatments when the contaminant concentration is low.[11] Of the photocatalytic semiconductor oxides, titanium dioxide is the most commonly employed due to its numerous favorable properties. It has high stability and activity for a variety of photocatalytic reactions; it is widely available, inexpensive, and harmless to humans; and the wavelengths required to activate the photocatalyst are present in sunlight.[12,13]

A number of studies have examined the photocatalytic degradation of CH_2Cl_2 both in aqueous solution and in the gas phase. Liquid-phase experiments show that complete degradation of CH_2Cl_2 to HCl, CO_2, and Cl^- is achievable.[14−19] Photodegradation under anaerobic conditions can occur by direct oxidation to produce formic acid, formaldehyde, methanol, and chloride ion, although the reaction rate is slower than for CCl_4.[18] In the presence of oxygen, the degradation rate is increased, and the product distribution changes as well, strongly favoring CO_2 formation, while the methanol intermediate is not detected.[15,19] Chloride ion has been observed to impede the degradation.[14] In the gas-phase photooxidation of dichloromethane, significant quantities of phosgene ($COCl_2$), CO, Cl_2, and CCl_4 are produced, in addition to the major species HCl and CO_2.[20,21] Lichtin and co-workers have shown that water vapor impedes the degradation, such that at 3% humidity, the reaction rate is reduced by an order of magnitude and is similar to the aqueous phase rate.[20] It was also found that mixing dichloromethane with trichloroethylene can speed the degradation.[22,23] Trichoroethylene is much easier to degrade, and presumably produces chlorine radicals that can initiate CH_2Cl_2 degradation. Recent experiments by Lin and co-workers showed the importance of added oxygen to facilitate and accelerate the photodecomposition of methylene chloride to CO, carbonate, formate, water, and CO_2 as final products that were adsorbed to the TiO_2 surface.[24] In these experiments, the samples were evacuated prior to FTIR observation so that gas phase and weakly bonded species were not observed.

In a previous study, we reported significant changes in the reactivity of dichloromethane that depended on the nature of the irradiation source.[21] Using pulsed laser irradiation, the production of phosgene as an intermediate was completely suppressed. Dichloromethane degradation proceeded without oxygen as a co-reagent, most likely through a direct reduction process. In the present study, we report new findings on TiO_2 photocatalysis of dichloromethane using UV lamp irradiation using in situ FTIR and solid-state NMR (SSNMR) detection methods. Specifically, we report the presence of formyl chloride as a new intermediate and, under high oxygen concentrations, CO, HCl, $COCl_2$, $CHCl_3$, and CCl_4 are found to be long-lived intermediate species as opposed to final products. The reaction kinetics are complex and depend strongly on oxygen concentration. In particular, the dynamics of phosgene production under lamp irradiation indicate the participation of an additional chlorine radical source. SSNMR experiments show that a

* Corresponding authors. E-mail: raftery@purdue.edu, jfrancis@purdue.edu.

10.1021/jp037066b CCC: $27.50
Published on Web 04/14/2004

surface-bound chloromethoxyl species is formed when dichloromethane is adsorbed on anatase TiO_2. There appear to be two phosgene species formed at low oxygen concentrations, which further contributes to the complexity of the reaction kinetics.

Experimental Section

FTIR Studies. CH_2Cl_2 (Mallinckrodt, 99.5%) was purified by vapor pressure distillation on a vacuum rack, while compressed oxygen (Airco and BOC Gases) was used without further purification. Experiments were carried out under static reaction conditions in a home-built Pyrex glass reaction chamber equipped with ZnSe or NaCl IR windows, as well as a quartz window for UV light transmission.[21] A crossed-beam arrangement was employed to allow in situ monitoring of the reactions. The reaction cell was mounted inside a Mattson Galaxy Series 7000 FT-IR equipped with a MCT detector. Spectra were obtained in the mid-IR range of 4000 to 650 cm^{-1} at a resolution of 1 cm^{-1}. Sixteen transients were acquired per spectrum to provide a good balance between signal-to-noise and decent time resolution. The method used for constructing and coating the catalyst's support was adapted from Yates and co-workers.[13,25,26] A slurry was made by suspending 1.0 g of TiO_2 (Degussa P-25, 70% anatase and 30% rutile, 55 m^2/g) in 10 mL of H_2O and 90 mL of acetone, and sonicating for approximately 45 min. The slurry was then sprayed onto a 2 cm^2 tungsten mesh (Unique Wire) using a Kontes nebulizer. Approximately 20 mg of TiO_2 was coated on the support mesh. Afterward, the TiO_2-coated mesh was heated at 500 °C in the presence of O_2 (by passing a current through the wire mesh) for 10 h to destroy any organic contaminants. The mesh was positioned in one of two orientations during the reaction studies. By aligning the mesh perpendicular to the UV source and parallel to the IR source, light reflections from the irradiation source into the instrument's detector could be minimized. This orientation was used to study gas-phase species. Alternatively, the mesh could be aligned at 45 degrees to both the IR and UV beams, which allowed IR spectra to be taken of both the gas- and surface-phase species. After the catalyst was prepared, desired amounts of O_2 and CH_2Cl_2 were loaded into an evacuated reagent manifold and equilibrated for about 1 h. The partial pressure of CH_2Cl_2 in all cases was 2.8 to 3.6 Torr, with O_2/CH_2Cl_2 ratios ranging from 0.30 to 11, as measured in the manifold after mixing occurred. During this equilibration period, the mesh was resistively heated under high vacuum to 110 °C for 30 min. The cell was allowed to cool to room temperature, where a base pressure of 10^{-5} Torr could be achieved and a background scan of the empty chamber was taken. The chamber was then filled with the equilibrated reactant gases. An initial FT-IR scan was acquired to determine reagent purity, and data were taken at regular intervals during the photoreactions to monitor intermediates and products. A 300 W Xe arc lamp (ILC Technology Inc.) was used as the UV source for these experiments, and was operated at roughly 280 W total output. A water IR cell and heat-absorbing filter (KG1 Schott type) were used to reduce IR heating effects, and a UV-cutoff filter (WG295 Schott type) was used to avoid any direct-photolysis reactions. This left approximately 2.1 W of filtered radiation (Scientech power meter) to enter the reaction chamber. After the reaction was complete, the mesh was removed from the chamber and the preparation was repeated for the next experiment.

SSNMR Studies. The adsorption of dichloromethane on Degussa P-25 TiO_2 powder and the two parent oxides, pure anatase (Hombikant UV 100), and rutile (Alfa Æsar) TiO_2 powders, and the photooxidation of dichloromethane on Degussa P-25 TiO_2 powder were studied using SSNMR. Table 1 gives information on the catalysts, morphologies, surface areas, and masses used in the NMR experiments. Each sample was prepared in a 5 mm NMR tube. The mass of TiO_2 powder given in Table 1 was packed into an NMR tube and attached to a vacuum manifold. The catalyst was then pretreated by heating the catalyst under a vacuum of approximately 5×10^{-5} Torr at 773 K for 4 h, and then calcined with less than one atm of dry O_2 at 773 K for 4 h. Once the heating cycle was complete, the catalyst was once again evacuated to a pressure of 5×10^{-5} Torr. After pretreatment, the catalyst was loaded with 48 μmol of ^{13}C-labeled dichloromethane ($^{13}CH_2Cl_2$, Cambridge Isotope Laboratories), and either 96 or 240 μmol of O_2 using a liquid nitrogen trap, and then flame sealed 10−12 mm above the catalyst. In situ NMR experiments were performed using a home-built optical/magic angle spinning (MAS) probe and light delivery system.[27] The probe was doubly tuned for ^{1}H and ^{13}C observation at frequencies of 300 and 75.4 MHz, respectively, using a Varian Inova spectrometer. The probe is capable of spinning the sealed NMR samples at speeds as high as 2.7 kHz. Light from the 300 W Xe arc lamp (ILC Technology) was delivered to the sample region inside the magnet via a liquid-filled optical light guide (Oriel Corp.). The wavelength of light delivered to the sample was selected by the use of dichroic mirrors (Oriel Corp.) attached to the Xe arc lamp. In this case, a dichroic mirror that passed light with wavelengths between 350 and 450 nm was used. A 70 mm long polished suprasil quartz rod was attached to the end of the light guide to reduce radio frequency pickup by the probe coil from the aluminum-encased light guide. The light from the quartz rod quickly diverged to cover the entire sample region. The near-UV light power that reached the sample was measured to be 5 mW by standard ferrioxalate actinometry.[28]

TABLE 1: TiO_2 Catalyst Morphology, Surface Area, and Mass Used in Dichloromethane Adsorption Experiments, and the Chemical Shift of Dichloromethane on the Various Catalysts

catalyst	morphology	surface area ($m^2\,g^{-1}$)	mass used (mg)	chemical shift (ppm)
Hombikant UV 100	anatase	>250	140	60
Alfa Æsar	rutile	3.3−6.1	304	58
Degussa P-25	70% anatase 30% rutile	55	180	54
Liquid[a]				53.7

[a] *Sadtler Standard Carbon-13 NMR Spectra*; Bio-Rad Laboratories: Philadelphia, PA, 1994.

Results and Discussion

Adsorption Studies. The adsorption of dichloromethane on Degussa P-25, pure anatase, and rutile TiO_2 powders was studied using ^{1}H-^{13}C cross-polarization NMR experiments coupled with magic angle spinning (CP/MAS) with a 0.35 ms CP contact time. Chemisorbed molecules are easily distinguished from physisorbed or gaseous molecules using CP/MAS experiments because the CP/MAS spectrum is influenced significantly by the mobility of molecules due to its effect on ^{1}H-^{13}C dipolar coupling. Figure 1 shows the ^{13}C CP/MAS NMR spectra of dichloromethane adsorbed on (a) pure anatase (Hombikant UV 100), (b) Degussa P-25, and (c) pure rutile (Alfa Æsar) TiO_2 powders. The chemical shift of dichloromethane varies from 54 ppm on the rutile powder to 60 ppm on the anatase powder (Table 1). In each case, the resonance line corresponding to

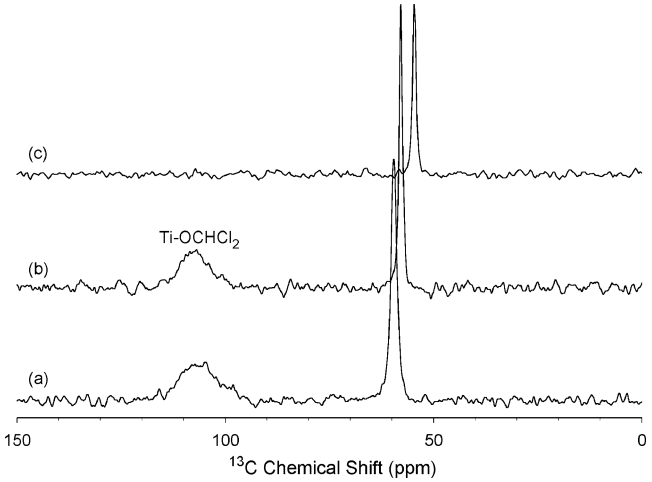

Figure 1. Proton-decoupled ^{13}C CP/MAS NMR spectra of dichloromethane adsorbed on (a) anatase, (b) Degussa P-25, and (c) rutile TiO_2 powders.

dichloromethane is relatively narrow, indicating that dichloromethane is reasonably mobile on the TiO_2 surface. The variance in chemical shift is due to differences in surface properties including the surface area and morphology of each of the catalysts. A broad resonance appears at approximately 105 ppm on the pure anatase and Degussa P-25 TiO_2 catalysts. The surface species responsible for this resonance is identified as a Ti-bound dichloromethoxy species ($Ti-OCHCl_2$), which is formed by the reaction of dichloromethane with the TiO_2 surface. The formation of surface-bound chloromethoxy groups has been observed previously in adsorption studies of chloromethane on alumina surfaces,[29] acidic, basic, and neutral FAU type zeolites,[30] and dichloromethane on γ-Al_2O_3.[31] For example, the adsorption of chloromethane, dichloromethane, and chloroform on zeolite ZnY was studied using SSNMR.[32] The isotropic ^{13}C chemical shift of a dichloromethoxy species which was bridge bonded to a Si and an Al atom was observed to be 95 ppm. This value is somewhat different from that measured on TiO_2 powder (105 ppm); however, the ^{13}C chemical shift of a surface-bound species varies drastically depending on the identity of the metal cation present in the sample, and has been demonstrated in the variation in chemical shift of the metal bound ethoxide species.[32] Therefore, the substitution of Ti for Si or Al can result in a change in chemical shift of the dichloromethoxy surface species. The dichloromethoxy species was not observed on the rutile TiO_2 catalyst; however, we can attribute this to the low surface area of the rutile catalyst.

Photooxidation Studies. In situ photooxidation studies were carried out using both FTIR and SSNMR detection methods under a variety of conditions. Representative IR spectra are shown in Figure 2 for the photocatalytic oxidation of 3.6 Torr of CH_2Cl_2 and 6.7 Torr of O_2. Well-resolved spectral features for a variety of species are evident in the spectra. A number of intermediates and final products are observed, including CO, phosgene, HCl, CH_3Cl, and final product CO_2. Generation of Cl_2 during the destruction of CH_2Cl_2 was also expected and has been shown to occur;[20] however, clearly Cl_2 cannot be observed using FTIR spectroscopy. Spectral assignments were made by comparison to literature values.[25,34] Observed IR peaks for the different species are tabulated in Table 2. These spectra give an overall picture of the temporal development for intermediate production and destruction.

A series of reactions were carried out under different concentrations of added oxygen, (0.9 to 32 Torr). In Figure 3, two representative kinetic plots of the reactions for O_2/CH_2Cl_2

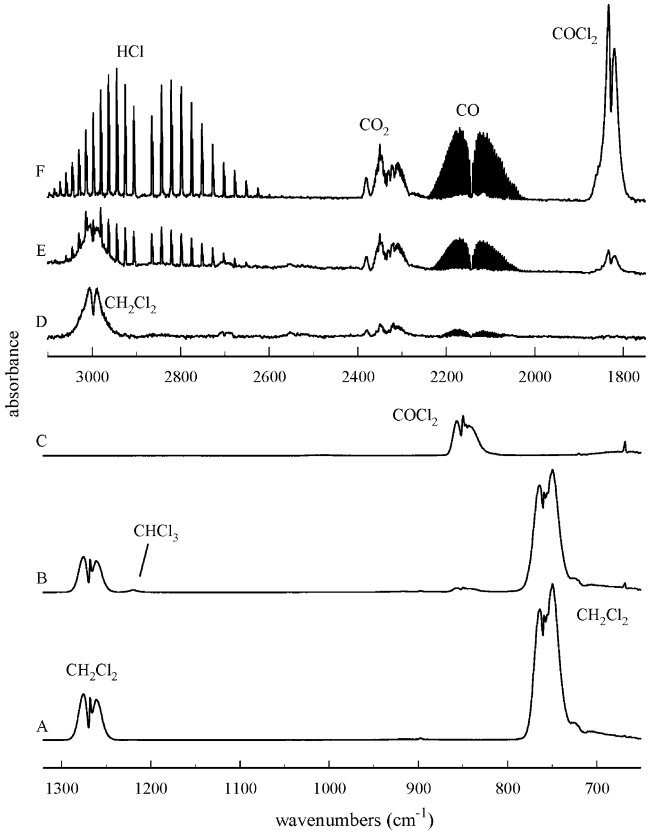

Figure 2. Representative FTIR spectra obtained during the photocatalytic degradation of CH_2Cl_2. (6.7 Torr O_2:3.6 Torr CH_2Cl_2) Spectra A−C: 1320 to 650 cm^{-1}; spectra D−F: 3100 to 1750 cm^{-1}.

TABLE 2: FTIR Wavelengths of Observed Species in the Photocatalytic Degradation of CH_2Cl_2

species	observed bands (cm^{-1})	mode description
CH_2Cl_2	2990	ν(C−H)
	1276	δ(C−H)
	785	ν_{as}(C−Cl)
CO_2	2349 (band center)	ν(C═O)
	667	$\delta(CO_2)$
CO	2144 (band center)	ν(CO)
$CHCl_3$	1219	δ(C−H)
	776	$\nu_{as}(CCl_3)$
HCl	2887 (band center)	ν(C−H)
$COCl_2$	1831	ν(C═O)
	1818	ν(C═O)
	849	$\nu(C-Cl_2)$
CCl_4	795	$\nu_{as}(C-Cl_4)$
CHOCl	2929	ν(C−H)
	1794	ν(C═O)
	1307	δ(C−H)
	739	$\nu_{umb}(C-Cl_2)$

ratios of 1.9 (6.7 Torr O_2, 3.6 Torr CH_2Cl_2) and 10.8 (31.7 Torr O_2, 3.0 Torr CH_2Cl_2) are shown. Due to the different adsorption propensities of the various intermediates and products, whose IR absorptivities change upon adsorption to the catalyst surface, it was difficult to quantitate the different species using these IR data alone. In principle, NMR experiments should be able to provide quantitative data for the oxidation of dichloromethane, as we have shown in previous photocatalytic studies.[27] However, the carbon containing intermediate species, $CHCl_3$, $COCl_2$, and CO, are formed in very small quantities which makes quantitation difficult. In addition, CCl_4 was below the detection limit in the NMR experiments. Due to the difficulty in determining the concentrations of the species, kinetic data for the IR peak

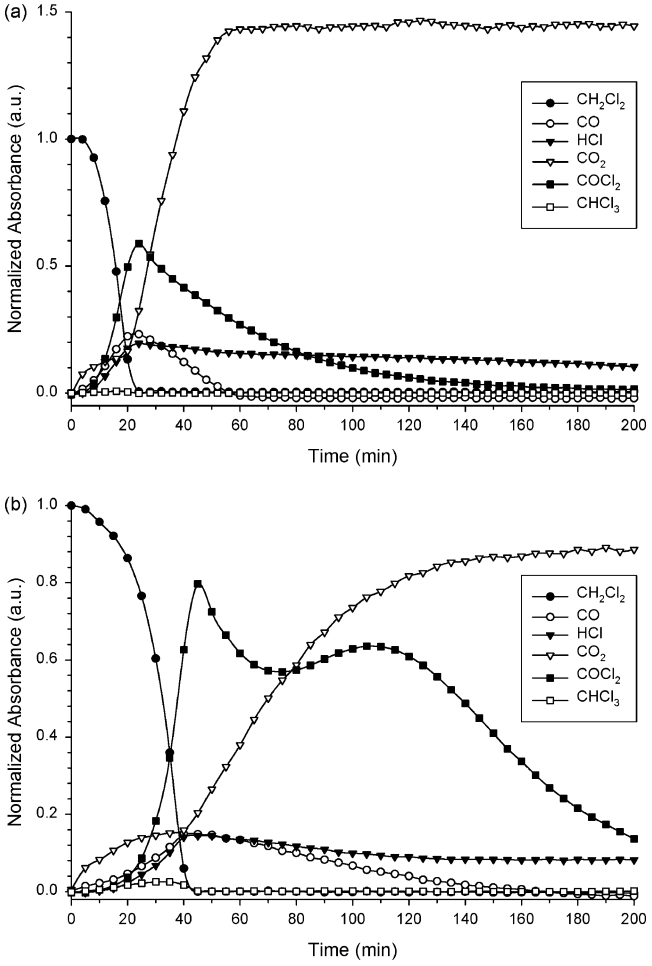

Figure 3. Kinetic plot for the photocatalytic destruction of CH_2Cl_2 at an O_2/CH_2Cl_2 ratio of (a) 10.8:1, and at (b) 1.9:1.

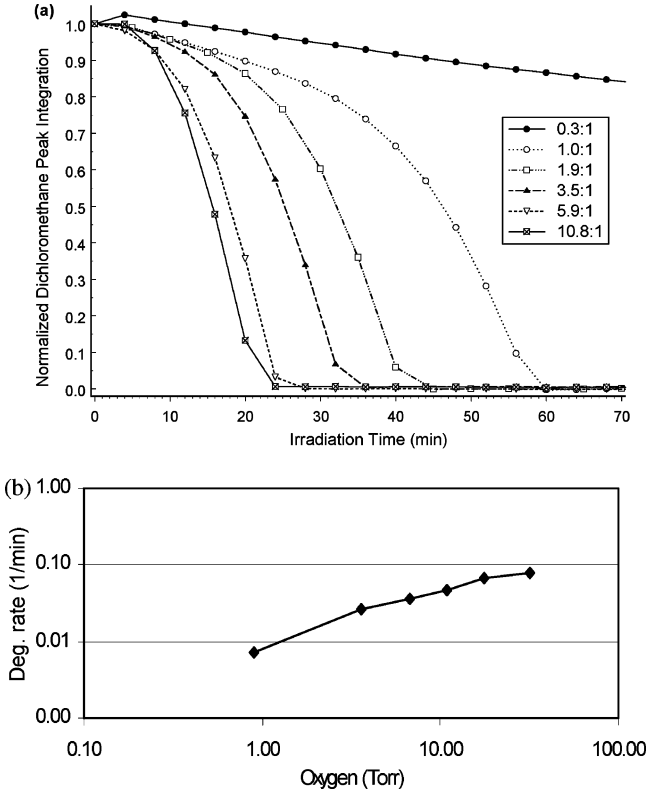

Figure 4. Oxygen dependence on the degradation rate of CH_2Cl_2: (a) kinetic plot showing the degradation of CH_2Cl_2 at six different oxygen concentrations, and (b) rate of degradation of CH_2Cl_2 versus O_2 concentration.

intensities are scaled via peak integration using the initial CH_2Cl_2 peak area as a reference.

As can be seen by comparing the two reactions in Figure 3, the reaction dynamics of dichloromethane depend strongly on the oxygen concentration. For example, the CH_2Cl_2 degradation rate increases significantly as a function of oxygen concentration, and is evidently a very nonlinear function of reaction time (Figure 4(a)). The accelerating reaction rate is observed at all but the lowest oxygen concentration, and occurs roughly at the same point in the reaction (in terms of % degraded), which is a strong indication of the participation of radical chain reactions. Most likely, chlorine radicals play an important role in the observed reactions, as they do in the photocatalytic degradation of trichloroethylene[35,36] and would thus give rise to the observed nonlinear CH_2Cl_2 degradation rates. In other studies of dichloromethane degradation, a change in the rate of photooxidation of dichloromethane was observed with respect to oxygen concentration. Two mechanisms were proposed for the destruction of dichloromethane, namely, oxidative attack and reduction, with oxidative attack being the more rapid mechanism for the destruction of dichloromethane.[20,24] When the degradation rate is plotted versus oxygen concentration (Figure 4(b)), it can be seen that the rate shows a considerable dependence on oxygen concentration at the lower oxygen pressures. However, as the oxygen pressure is increased, the degradation rate levels off and becomes relatively independent of the oxygen concentration. A similar oxygen dependence was observed in the photooxidation of 2-methylbutane[37] and 2-propanol[38] over TiO_2. The authors in those studies ascribed this oxygen dependence to the importance of O_2 adsorption at the lower concentrations, which begins to saturate at the higher O_2 pressures.

FTIR studies also showed that a change in the dynamics of CO and HCl is evident when the oxygen concentration is varied. At very low oxygen content (0.3 O_2:CH_2Cl_2) CO is a persistent intermediate even after several hours of irradiation, as seen in our previous study.[21] However, as the relative amount of oxygen increases (Figure 5(a)), CO is found to be truly intermediate in nature. It is converted to CO_2 in the presence of excess O_2. CO has also been observed as an intermediate in the photooxidation of CH_3Cl on TiO_2 powder and was completely oxidized to CO_2 after a prolonged period of irradiation (>500 min).[13] Lin and co-workers also observed the conversion of CO to CO_2 in the presence of O_2.[24] The destruction of another dichloromethane degradation product, HCl, has also been observed at high oxygen concentrations (Figure 5(b)). Hydrochloric acid is often thought to be a final product in the photocatalysis of a number of chlorinated VOCs.[25,35,39,40] At low relative oxygen concentrations, HCl indeed appears to be a final product in the photooxidation of CH_2Cl_2. However, as oxygen concentrations rise, it is evident that even this stable acid is eventually destroyed. Since the IR spectra obtained at long reaction times for the high O_2 concentration experiments indicate the presence of CO_2, H_2O, and some residual HCl, it is likely that Cl_2 is produced or Cl reacts with exposed surface Ti atoms, producing a metal oxo-chloride.[41,42] Recent experiments on single-crystal TiO_2 surfaces have indicated the formation of exposed, individual Cl atoms.[43] As a result, the TiO_2 surface can act as both a sink for and source of reactive Cl radicals. The kinetic plot for the formation and destruction of HCl at the highest O_2 concentration (10.8 O_2/CH_2Cl_2) exhibits a nonexponential decay which may indicate that the surface sites involved in the destruction of HCl are occupied by other surface species, such

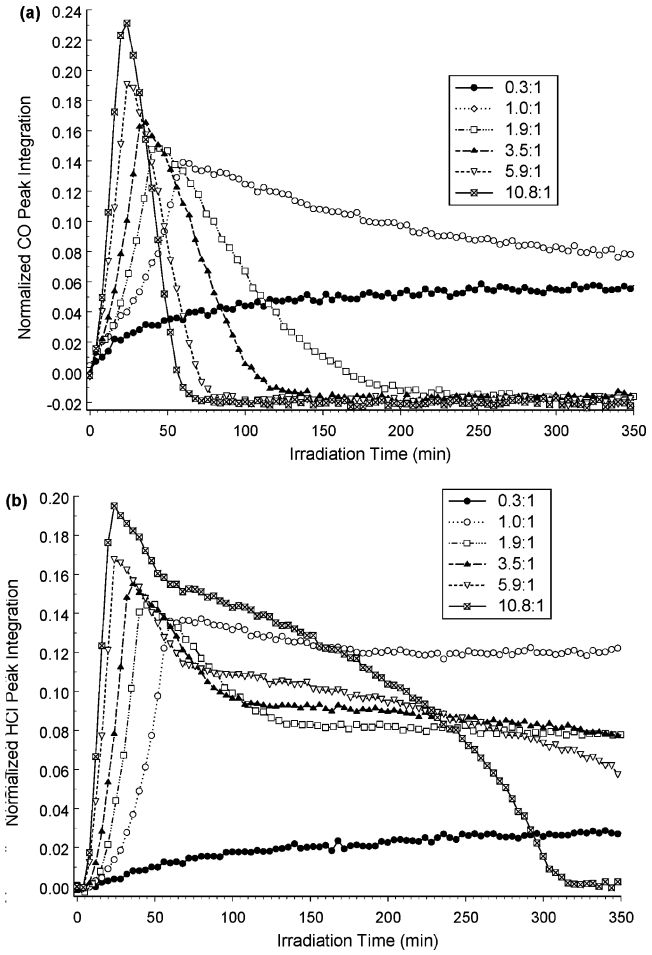

Figure 5. Kinetic plots of the formation and degradation of (a) CO and (b) HCl at six different oxygen concentrations.

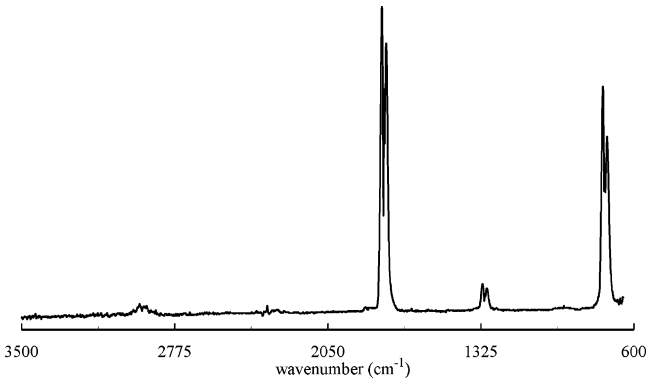

Figure 6. FTIR spectrum of formyl chloride (CHOCl) discovered as a short-lived intermediate at high oxygen concentrations.

as Cl. Alternatively HCl may be formed from the destruction of other long-lived chlorine-containing species such as phosgene.

Experiments run under higher O_2 concentrations gave rise to the observation of a new intermediate in the reaction. The new intermediate contained IR absorption peaks at 2929, 1794, 1307, and 739 cm^{-1}; however, these peaks are obscured by overlapping peaks from HCl, $COCl_2$, and CH_2Cl_2. The spectrum shown in Figure 6 was obtained by subtracting calibration spectra for CH_2Cl_2, CO, phosgene, CO_2, and HCl from an experimental scan. After comparing the IR transitions against literature values,[44] we find that the spectrum corresponds to formyl chloride (CHOCl). Formyl chloride is a logical intermediate in the reactions of methylene chloride, but prior to these experiments had not been reported in TiO_2 photocatalytic

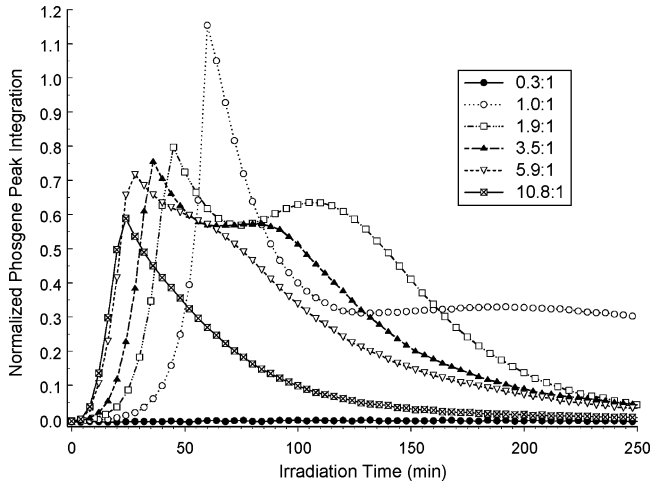

Figure 7. Formation and destruction of phosgene at six different O_2 concentrations.

reactions. Formyl chloride can be easily overlooked because it typically arises at the same time as phosgene (1827 cm^{-1}), and its absorption band falls in the region of H_2O absorption (broad absorption centered at 1595 cm^{-1}). Although the formation of formyl chloride was detected shortly after phosgene, formyl chloride appears to be a product of dichloromethane oxidation instead of that of a different intermediate such as phosgene because formyl chloride was no longer detected after dichloromethane had been completely oxidized and plenty of phosgene persisted. Kinetic plots for formyl chloride are difficult to obtain because calibrated values for the integrated intensities of CH_2Cl_2, CO, phosgene, CO_2, and HCl must be subtracted from the experimental spectra at each data point.

Two minor products, chloroform and carbon tetrachloride, were also observed as intermediates in the destruction of CH_2Cl_2. $CHCl_3$ appears immediately after irradiation, and is quickly consumed (within 5 min) after the methylene chloride concentration goes to zero. This behavior is observed at all oxygen concentrations. The amount of chloroform produced decreased as the oxygen concentration in the sample was increased. Carbon tetrachloride was also observed, particularly at low oxygen concentrations. As the oxygen concentration was raised, CCl_4 was found to be intermediate in nature and was degraded. CCl_4 was not observed at long reaction times for reactions run under high oxygen concentrations. The formation of $CHCl_3$ and CCl_4 from CH_2Cl_2 again suggests that a free radical mechanism involving chlorine radicals is involved in the destruction of CH_2Cl_2. The formation of CH_2Cl_2 from CH_3Cl has previously been described using a free-radical-mediated mechanism involving reaction of methoxy radicals generated from peroxide species with chlorine radicals.[13]

Phosgene formation and destruction also shows a dependence on the relative amount of oxygen available. Figure 7 shows the formation and destruction of phosgene at six different O_2 concentrations. Overall, phosgene production is reduced as oxygen concentration is increased. Of special interest is a second production channel for phosgene at lower oxygen concentrations. This is evidenced by a second, local maximum in the kinetic plot for phosgene in the photocatalytic oxidation experiment using an O_2/CH_2Cl_2 ratio of 1.9:1. The local maximum is observed at approximately 110 min, some time after its global maximum concentration. This second production channel is less prominent as the oxygen concentration is increased.

To better understand the phosgene kinetics in the photooxidation of dichloromethane using Degussa P-25 TiO_2 powder,

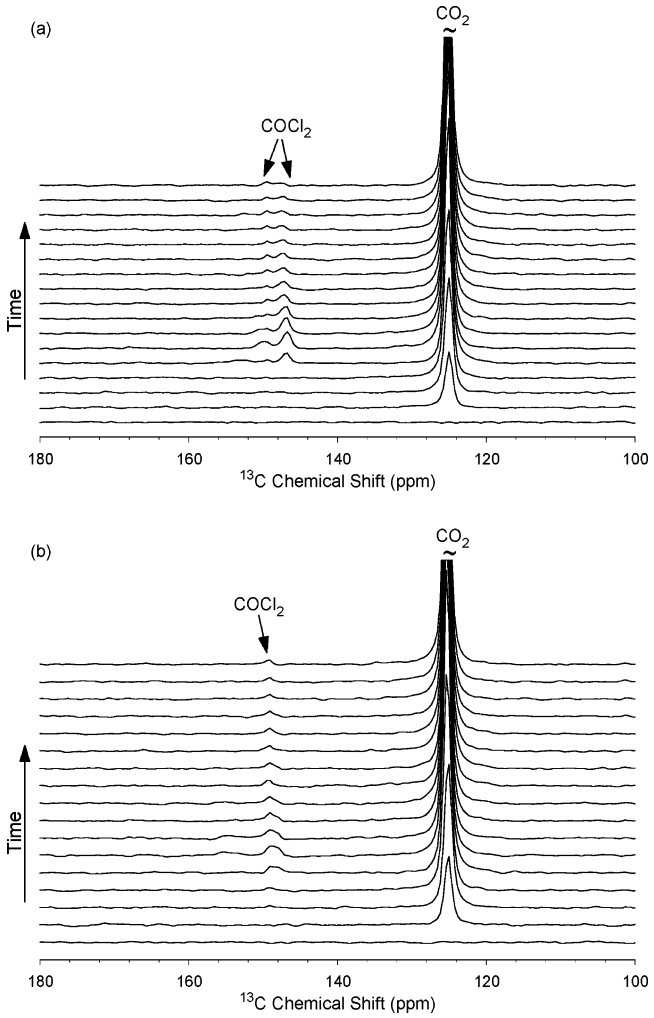

Figure 8. Proton-decoupled ^{13}C Bloch decay spectra showing the time progression of the photooxidation of dichloromethane on Degussa P-25 TiO_2 powder with (a) 2:1 and (b) 5:1 O_2 to dichloromethane concentration ratios.

in situ SSNMR experiments were carried out using 96 μmol and 240 μmol of O_2. Figure 8 shows the time progression over a 180 min period for the photooxidation of dichloromethane with an O_2/CH_2Cl_2 concentration ratio of (a) 2:1 and (b) 5:1. The intermediates CO (183.6 ppm), trichloromethane (78.5 ppm), phosgene (146.7 and 150.0), and gas-phase CH_2Cl_2 at 54.6 ppm were observed, as well as the final product CO_2 (125.1 ppm). Two unique phosgene resonances are clearly observed in the sample prepared with a lower O_2 concentration (Figure 9). The resonances at 146.7 and 150.0 ppm are assigned to gas-phase and adsorbed phosgene, respectively.[27] However, the kinetics of phosgene formation and oxidation could not be studied in depth using in situ SSNMR experiments because of the low quantities of phosgene produced during the reaction (<6% of the original dichloromethane signal). In agreement with the FTIR experiments, the total amount of phosgene produced in the in situ SSNMR studies decreased as the O_2 concentration was increased. As shown in Figure 8, the amount of the surface-bound phosgene (150.0 ppm) decreased as the O_2 concentration in the sample was increased.

There are two possible explanations for the formation of the second, surface-bound phosgene species. First, the formation of a second phosgene species at lower oxygen concentrations indicates that lattice oxygen may participate in the formation of the second phosgene species. TPD studies of the photodestruction of CCl_4 on an ^{18}O-labeled MgO surface have shown

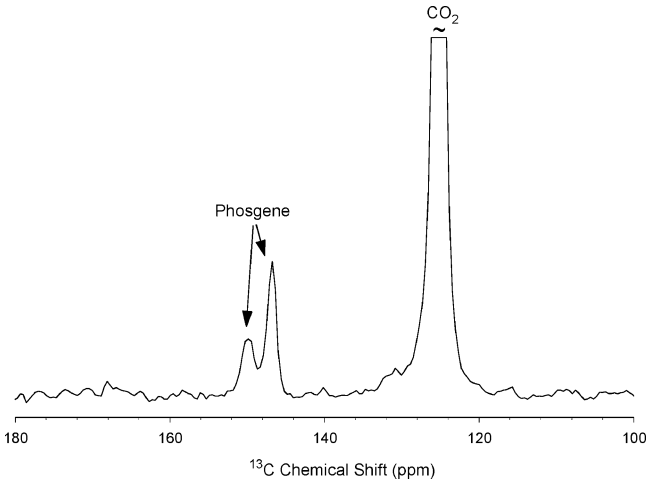

Figure 9. Proton-decoupled ^{13}C Bloch decay spectra obtained after 50 min of in situ UV irradiation of 48 μmol of dichloromethane and 96 μmol of O_2 on Degussa P-25 TiO_2 powder.

that lattice oxygen is involved in the formation of phosgene on dehydrated MgO surfaces when no O_2 is present.[45] At higher O_2 concentrations, there is an abundance of O_2 present in the sample, and strongly bound lattice oxygens are less likely to participate in the formation of phosgene as is reflected in the decrease in the amount of adsorbed phosgene observed in Figure 8(b) and in the decrease in the amount of phosgene produced by the second reaction channel in the FTIR studies. A second possible explanation for the presence of the surface-bound phosgene species is the reaction of CO with another source of Cl, such as Cl_2, or a surface source of chlorine, such as adsorbed chlorine or metal-ligated chlorine atoms. Metallo-chlorates are known to exchange chlorine relatively easily, depending on surface conditions such as temperature and water content.[46] Our FTIR studies showed that the phosgene concentration increased during the collapse of intensity in the CO and HCl bands; however, irradiation of CO, O_2, and HCl over TiO_2 did not result in the formation of phosgene. Nevertheless, it has been shown that phosgene is formed when mixtures of CO, Cl_2, and O_2 are illuminated.[47]

Finally, the overall reaction kinetics and product distribution were also examined as a function of the excitation wavelength and power. Using a series of short wavelength cutoff filters in the range of 245 nm to 435 nm, it was observed that the use of the longer wavelength cutoff filters served to slow the reaction rate, such that at 435 nm and longer wavelengths, very little methylene chloride was degraded. This is to be expected as the cutoff filters served to reduce the flux of supra-band gap photons. However, the product distribution was largely unaffected. This result indicates that no direct, gas-phase photolysis of methylene chloride or second reaction mechanism is occurring that would give rise to a second, different reaction channel. Similar results were obtained by varying the lamp power, holding the oxygen concentration fixed. Data from these studies is available in the Supporting Information.

Conclusions

The photocatalytic oxidation of dichloromethane has been studied in detail on several TiO_2 catalysts using in situ FTIR and SSNMR methods. After adsorption, dichloromethane can form a surface-bound chloromethoxy species on anatase TiO_2 powder. The rate of CH_2Cl_2 photooxidation has a pronounced oxygen dependence and results in significantly shorter destruction times at high relative O_2 concentrations. At elevated oxygen

concentrations, CO, HCl, and CCl_4 formed in the reactions are found to be long-lived intermediates and not final products as previously observed. The concentrations of the carbon-containing intermediate species are found to be low using SSNMR experiments. At high oxygen concentrations, formyl chloride was observed as a new species in the degradation of methylene chloride. Finally, there appear to be at least two pathways leading to the formation of phosgene. The first pathway results directly from the degradation of CH_2Cl_2, while the second occurs concurrently with the rapid conversion of CO to CO_2. SSNMR experiments show that the two distinct phosgene species can be attributed to gas-phase and surface-bound phosgene. It is believed that lattice oxygen and possibly surface chlorine species are involved in the formation of the second surface-bound phosgene species.

Acknowledgment. The authors thank the AT&T/Lucent Technologies Industrial Ecology Faculty Fellowship program, the National Science Foundation (CHE 97-33188, CAREER Grant), and the donors of the Petroleum Research Fund, administered by the American Chemical Society for supporting this research.

Supporting Information Available: Additional NMR spectra of dichloromethane photooxidation, FTIR spectra of formyl chloride formation, and FTIR power and wavelength-dependent studies. This material is available free of charge via the Internet at http://pubs.acs.org.

References and Notes

(1) Freeman, H. M. *Incinerating Hazardous Wastes*; Technomic Publishing Co.: Lancaster, PA, 1988; p 375.
(2) Patterson, J. W. *Industrial Wastewater Treatment Technology*, 2nd ed.; Butterworth Publishers: Boston, 1985.
(3) MacDonald, J. A.; Kavanaugh, M. C. *Environ. Sci. Technol.* **1994**, *28*, 326A.
(4) Buonicore, A. J.; Davis, W. T. *Air Pollution Engineering Manual*; Air & Waste Management Association, Van Nostrand Reihold: New York, 1992.
(5) Derenzo, D. J. *Biodegradation Techniques for Industrial Organic Wastes*; Noyes Data Corporation: Park Ridge, NJ, 1980; p 358.
(6) *Photocatalysis and Environment*: *Trends and Applications*, Schiavello, M., Ed.; Kluwer Academic Publishers: Dordrecht, 1988.
(7) *Photocatalytic Purification and Treatment of Water and Air*; Ollis, D. F., Al-Ekabi, H., Eds.; Elsevier: Amsterdam, 1993.
(8) Fox, M. A.; Dulay, M. T. *Chem. Rev.* **1993**, *93*, 341.
(9) Linsebigler, A. L.; Lu, G.; Yates, J. T. *Chem. Rev.* **1995**, *95*, 735.
(10) Hoffmann, M. R.; Martin, S. T.; Choi, W.; Bahnemann, D. W. *Chem. Rev.* **1995**, *95*, 69.
(11) Miller, R. Proceedings of the 1st International EPRI/NSF Symposium in Advanced Oxidation; EPRI TR-102927-V2, Electric Power Research Institute: Palo Alto, 1993; pp 2−27 to 2−28.
(12) Pourbaix, M. *Atlas of Electrochemical Equilibria in Aqueous Solutions*; Franklin, J. A., Ed; Pergramon Press: New York, 1966.
(13) Wong, J. C. S.; Linsebigler, A.; Lu, G.; Fan, J.; Yates, J. T., Jr. *J. Phys. Chem.* **1995**, *99*, 335.
(14) Hsiao, C.-Y.; Lee, C.-L.; Ollis, D. F. *J. Catal.* **1983**, *82*, 418.
(15) Tanguay, J. F.; Suib, S. L.; Coughlin, R. W. *J. Catal.* **1989**, *117*, 335.
(16) Halmann, M.; Hunt, A. J.; Spath, D. *Sol. Energy Mater. Sol. Cells* **1992**, *26*, 1.
(17) Sabin, F.; Türk, T.; Vogler, A. *J. Photochem. Photobiol. A: Chem.* **1992**, *63*, 99.
(18) Calza, P.; Minero, C.; Pelizzetti, E. *Environ. Sci. Technol.* **1997**, *31*, 2198.
(19) Calza, P.; Minero, C.; Pelizzetti, E. *J. Chem. Soc., Faraday Trans.* **1997**, *93*, 3765.
(20) Lichtin, N. N.; Avudaithai, M. *Environ. Sci. Technol.* **1996**, *30*, 2014.
(21) Miller, M.; Borisch, J.; Raftery, D.; Francisco, J. S. *J. Am. Chem. Soc.* **1998**, *120*, 8265.
(22) Lichtin, N. N.; Avudaithai, M.; Berman, E.; Grayfer, A. *Sol. Energy* **1996**, *56*, 377.
(23) Lichtin, N. N.; Avudaithai, M.; Berman, E.; Dong, J. *Res. Chem. Intermed.* **1994**, *20*, 755.
(24) Chen, M.-T.; Lien, C.-F.; Liao, L.-F.; Lin, J.-L. *J. Phys. Chem. B* **2003**, *107*, 3837.
(25) Fan, J.; Yates, J. T., Jr. *J. Am. Chem. Soc.* **1996**, *118*, 4686.
(26) Basu, P.; Ballinger, T. H.; Yates, J. T., Jr. *Rev. Sci. Instrum.* **1998**, *59*, 1321.
(27) Hwang, S.-J.; Petucci, C.; Raftery, D. *J. Am. Chem. Soc.* **1998**, *120*, 4388.
(28) Hatchard, C. G.; Parker, C. A. *Proc. Royal Soc. London* **1956**, *A235*, 518.
(29) Beebe, T. P., Jr.; Crowell, J. E.; Yates, J. T., Jr. *J. Phys. Chem.* **1988**, *92*, 1296.
(30) Kónya, Z.; Hannus, I.; Kiricsi, I. *Appl. Catal. B: Environ.* **1996**, *8*, 391.
(31) van der Brink, R. W.; Mulder, P.; Louw, R.; Sinquin, G.; Petit, C.; Hindermann, J.-P. *J. Catal.* **1998**, *180*, 153.
(32) Krawietz, T. R.; Goguen, P.; Haw, J. F. *Catal. Lett.* **1996**, *42*, 41.
(33) Pilkenton, S.; Xu, W.; Raftery, D. *Anal. Sci.* **2001**, *17*, 125.
(34) Sadtler Infrared Prism Spectra; Sadtler Research Laboratories, Inc.: Philadelphia, PA 1992.
(35) Nimlos, M. R.; Jacoby, W. A.; Blake, D. M.; Milne, T. A. *Environ. Sci. Technol.* **1993**, *27*, 732.
(36) Hung, C. H.; Marinas, B. J. *Environ. Sci. Technol.* **1997**, *31*, 562.
(37) Djeghri, N.; Teichner, S. J. *J. Catal.* **1980**, *62*, 99.
(38) Larson, S. A.; Widegren, J. A.; Falconer, J. L. *J. Catal.* **1995**, *157*, 611.
(39) Yamazaki-Nishida, S.; Cervera-March, S.; Nagano, K. J.; Anderson, M. A.; Hori, K. *J. Phys. Chem.* **1995**, *99*, 15814.
(40) Driessen, M. D.; Goodman, A. L.; Miller, T. M.; Zaharias, G. A.; Grassian, V. H. *J. Phys. Chem. B* **1998**, *102*, 549.
(41) Klabunde, K. J.; Stark, J.; Koper, O.; Mohs, C.; Park, D. G.; Decker, S.; Jiang, Y.; Lagadic, I.; Zhang, D. *J. Phys. Chem.* **1996**, *100*, 12142.
(42) Weckhuysen, B. M.; Mestl, G.; Rosynek, M. P.; Krawietz, T. R.; Haw, J. F.; Lunsford, J. H. *J. Phys. Chem. B* **1998**, *102*, 3773.
(43) Diebold, U.; Hebenstreit, W.; Leonardelli, G.; Schmid, M.; Varga, P. *Phys. Rev. Lett.* **1998**, *81*, 405.
(44) Hisatsune, I. C.; Heicklen, J. *Can. J. Spectrosc.* **1973**, *18*, 77.
(45) Zhou, X.-L.; Cowin, J. P. *J. Phys. Chem.* **1996**, *100*, 1055.
(46) Sosnov, E. A.; Malkov, A. A.; Malygin, A. A. *Russ. J. Appl. Chem.* **2000**, *73*, 1136.
(47) Ohta, T. *Bull. Chem. Soc. Jpn.* **1983**, *56*, 869.